



Health Risk Effects Associated with 5g Signal to the Member of the Public

Kefilwe Thoane, Risimati Dazmen Mavunda, Simon Connell,
Carrie Minnaar, Mhoyo-Di-Tamba Willie Vangu, Kayoda Dada,
Pathmanathan Naidoo and Dave Nichol

EasyChair preprints are intended for rapid
dissemination of research results and are
integrated with the rest of EasyChair.

February 1, 2024

HEALTH RISK EFFECTS ASSOCIATED WITH 5G SIGNAL TO THE MEMBERS OF THE PUBLIC

¹Department of Mechanical Engineering Science, University of Johannesburg, South Africa

² Nuclear Medicine, University of the Witwatersrand, South Africa

¹KT Thoane, ¹RD Mavunda, ¹SH Connell, ²C Minnaar, ²DTW Vangu, ²K Dada, ¹P Naidoo, ¹D, Nicholls

SUMMARY

The 5th generation (5G) communication system with an initial frequency below 6GHz can include the 26 -28 GHz bands often called millimeter wave (mmW), providing more capacity than the current 2G, 3G, and 4G RF signals. There is a public concern that 5G is harmful. Hence, scientific research is necessary to determine the potential of its benefits over the health risk effects. Ensuring the optimal performance, efficient spectrum utilization, and adherence to regulatory standards of 5G networks heavily relies on the accurate measurement and analysis of the intricate radiofrequency (RF) signals at their core. In this study, an assessment of electromagnetic radiation exposure was conducted at three distinct sample positions, precisely determined using GPS coordinates corresponding to celestial arrangements. The center frequency and span were carefully established to delineate the analysis range accurately. To ensure the utmost precision in our measurements, the resolution bandwidth (RBW) and video bandwidth (VBW) were meticulously configured. The signal frequency results of 3488.74 ± 20.60 MHz i.e., 3.5GHz from a direct digital modulation of an RF receiver for positions 1, 2, and 3, and the delta frequency of 1159.00 ± 21 b/s i.e., $1.2\text{Gb/s} \pm 21$ b/s were obtained. The average pulse time of 247 ± 57.07 ns. These results were within a low-power, wideband wireless of 1.2Gb/s as prescribed for the 5G range. The delta amplitude for the setup was -1.53 ± 2.81 db demonstrating a gain of RF reaching the receiver. The average specific absorption rate (SAR) in watts in this study for an average 60kg man was 0.08 W.kg^{-1} and does not exceed the SAR limits for general population/uncontrolled exposure of 0.08 W.kg^{-1} averaged over the whole body. A peak spatial-average SAR of 1.6 W.kg^{-1} over any 1 gram of tissue (defined as a tissue volume in the shape of a cube) for non-ionizing radiation workers. The conclusion of the study was that 5G RF at the base width 300MHz to 5GHz might not have an effect on the members of the public.

KEYWORDS

Radiofrequency, 5G signals, Radiofrequency, power density, spectrum analyzer, specific absorption rate.

1 INTRODUCTION

The advent of fifth-generation wireless technology, commonly known as 5G, has ushered in a new era of connectivity with unprecedented speed, capacity, and potential. As 5G networks continue to expand and evolve, the need for precise and comprehensive measurement of radiofrequency (RF) signals becomes increasingly paramount [1]. Accurate measurement and analysis of 5G RF signals are crucial not only for ensuring the optimal performance of these advanced networks but also for addressing concerns related to electromagnetic compatibility, spectrum efficiency, and potential health and safety considerations [2]. At the heart of this measurement process lies the indispensable tool known as the spectrum analyser. Spectrum analysers are sophisticated instruments designed to capture, analyse, and visualize the spectral characteristics of RF signals across a wide range of frequencies [3].

This exploration into the measurement of 5G RF signals and the utilization of spectrum analysers will delve into the fundamental concepts underlying RF measurement, the unique challenges posed by 5G technology, and the capabilities offered by modern spectrum analysers to address these challenges [4]. We will examine the various components that constitute 5G RF signals, including frequency bands, modulation schemes, and beamforming techniques, all of which contribute to the complexity of RF measurement. Moreover, we will explore how spectrum analyzers have evolved to accommodate the intricacies of 5G, offering advanced features such as real-time analysis, wide frequency coverage, and enhanced sensitivity.

From the precise identification of signal components to the detection of interference sources and the assessment of signal quality, spectrum analyzers have become indispensable tools in the ongoing development and optimization of 5G networks [5]. As the demand for faster and more reliable wireless communications continues to grow, the ability to effectively measure and analyze 5G RF signals will play a crucial role in shaping the future of wireless technology [6].

The 5G technology operates within the category of non-ionizing electromagnetic fields which cannot break down molecular bonds. A significant portion of the electromagnetic fields we encounter in our day-to-day existence arise from artificial sources, and it is worth noting that the majority of these fields fall under the category of non-ionizing radiation [7]. Throughout our lives, human beings have been continuously exposed to natural electromagnetic fields (EMF) [8]. Exposure limits vary based on the specific circumstances or factors involved in the specific type of electromagnetic field (EMF), and they are designed to incorporate substantial safety margins to provide additional protection [7].

Multiple concerns have emerged regarding the potential impact on health and safety due to the possibility of significantly increased exposure to radiofrequency electromagnetic radiation resulting from 5G technology [9]. Frequencies greater than 6 GHz have been utilized for decades in different applications such as radar,

microwave links, airport security screening, and medical treatments utilizing radiofrequency electromagnetic radiation [10]. Some potential health risks associated with 5G signals include increased exposure to electromagnetic radiation, which can lead to tissue damage and cancer. Other concerns include the potential for interference with other electronic devices and increased susceptibility to cyber-attacks. To date, most research regarding the impacts on the health of 5G signals has been conducted on animals or in laboratory settings, and there is restricted data on the long-term impact of 5G exposure on human health. As a result, it is difficult to make definitive conclusions about the risks associated with 5G signals. However, the use of millimeter waves by (5G) mobile networks, has caused an increase in public concern regarding potential issues. Potential health risks associated with 5G networks due to the higher frequency bands used.

2 LITERATURE REVIEW

Effective measurement of 5G RF signals is crucial due to the complex attributes of the technology. Spectrum analyzers have emerged as indispensable tools in this endeavor, providing a comprehensive framework to capture, visualize, and interpret RF signals [4]. The utilization of spectrum analyzers allows engineers and researchers to gain insights into signal behavior, interference patterns, and network efficiency, enabling efficient design, deployment, and maintenance of 5G networks.

The radio frequency spectrum comprises an infinite number of distinct frequencies that are represented as waves, with the wavelength of each wave corresponding to its frequency. The transfer of energy from one point to another through the movement of oscillating electric and magnetic fields in space is known as electromagnetic wave radiation. The wavelength (λ) of an electromagnetic wave is determined by its frequency (f) and propagation speed (v), which can be expressed using the following relationship:

$$\lambda = \frac{v}{f} \quad (1)$$

Radiofrequency exposure is commonly quantified as the radiofrequency energy flux per unit area, measured in watts of radiofrequency (RF) energy traversing a square meter of space (W/m^2) [6]. Alternatively, the intensity of radio waves can be expressed in terms of electric field intensity, which is measured in volts per meter (V/m) [6].

Radiofrequency (RF) exposure can be characterized using different parameters, including the strength of the electric field (E), magnetic field (H), power density (S), and specific absorption rate (SAR).

The Specific Absorption Rate (SAR) is described as the rate of energy absorption due to heating by a mass contained within a volume corresponding to a specific mass density. When taking into account living tissues or bodily organs. SAR is formulated as [7].

$$SAR = \frac{\sigma}{\rho} |E|^2, \quad [\text{W}/\text{kg}] \quad (2)$$

In this equation, the electrical conductivity is (σ) [S/m], while ρ [kg/m^3] denotes the density of a material, and represents the tissue or organ's density, with E [V/m] representing the internal electric field.

The electric field strength (E) denotes the measure of electric field intensity at a specific point in space and can be mathematically expressed as:

$$E = V/m \quad (3)$$

Where V is the voltage and m is the distance between two points.

Theoretically, RF exposure is based on the interaction between RF fields and biological tissue. When RF fields are absorbed by biological tissue, they can cause a rise in temperature due to the energy absorbed by the tissue. This can lead to tissue damage if the amount of energy absorbed is too high [6]. However, the majority of scientific evidence suggests that exposure to RF fields at levels typically encountered in daily life does not cause any detrimental health impacts. The guidelines set by organizations like the World Health Organization (WHO) and the International Commission on Non-Ionizing Radiation Protection (ICNIRP) are designed to ensure that exposure to radiofrequency (RF) fields remains below levels that could cause harm to human health.

Radiofrequency exposure is commonly quantified as the radiofrequency energy flux per unit area, measured in watts of radiofrequency (RF) energy traversing a square meter of space (W/m^2). Alternatively, the intensity of radio waves can be expressed in terms of electric field intensity, which is measured in volts per meter (V/m) [6]. These two metrics exhibit a mathematical relationship when examining locations that are several wavelengths away from the antenna or RF source. Specifically, the energy flux per unit area (S) is directly proportional to the square of the electric field intensity (E):

$$S (W/m^2) = [E (V/m)]^2 / [377(V^2/W)] \quad (4)$$

The assessment of health risk effects associated with 5G signals has been a topic of considerable interest and research. Numerous studies have been conducted to evaluate the potential health impacts of exposure to electromagnetic fields (EMF) emitted by 5G devices and infrastructure. While most of the scientific evidence suggests that 5G signals are unlikely to cause direct adverse health effects at the recommended exposure levels, there are ongoing debates and concerns regarding certain aspects [5].

The study was conducted to address a general concern that 5G RF has health effects on the members of the public by measuring the power density (dB) transmitted at the NASREC Sentech Macro base antenna; distribution antenna and active antenna unit (AAU) and, to assess the health effects on the members of the public and non-ionizing radiation workers who are exposed to 5G RF.

3 METHODOLOGY

The active antenna unit (AAU 5645) is a new type of RF module setup for a new radio (NR) network situated at the NASREC Sentec base station figure 1. The AAU5645 is one of Huawei's main products that implement massive MIMO in NR networks.

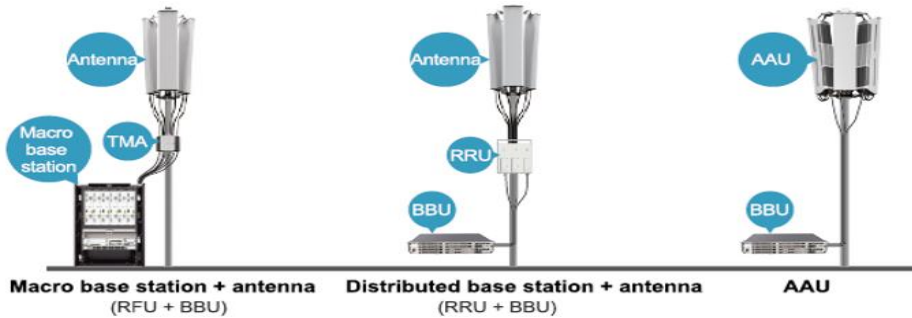


Figure 1 : Evolution of Huawei base stations [18]

The AAU5645 supports 64T64R. Through sharp increase to transmit and receive antenna channels, the system product provides greater diversity, array, spatial multiplexing, and interference suppression gains. This helps operators to maximize the use of the existing site and spectrum resources, enhance the system performance, and improve wireless network capacity.

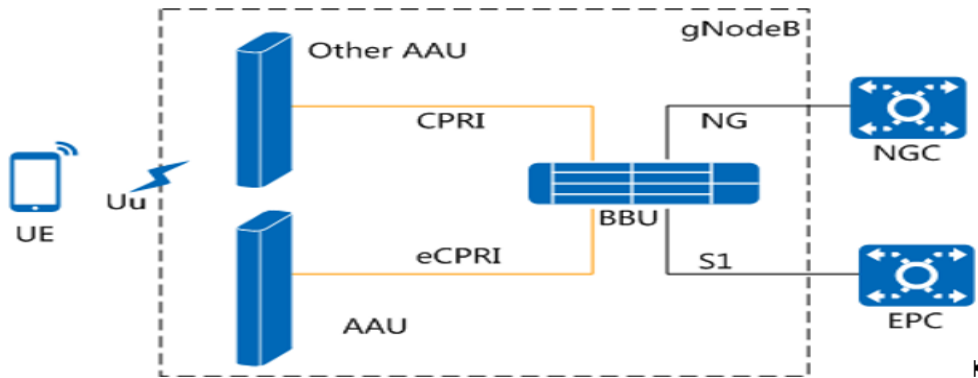


Figure 2: Position of the AAU5645 in the NR network [18]

The input RF signal AAU5645 was detected by an EXFO-FTB-1PRO system (Serial number: 1555113), in conjunction with an FTBX-88260 module (Serial Number: 1569346). Furthermore, the procedure encompassed the incorporation of an FR1 RF Transceiver Adapter (Serial Number: 1577341) and a Premium Sync Transceiver Adapter (Serial Number: 15237586) shown in figure 3.

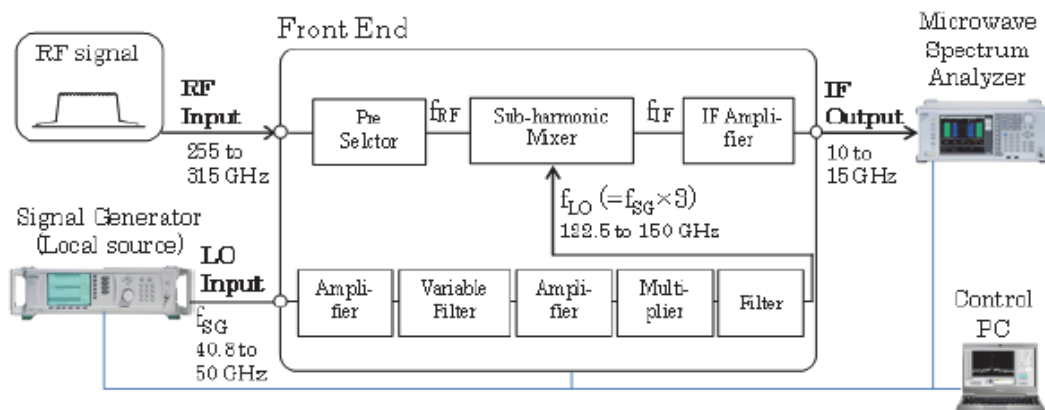


Figure 3 : 450MHz - 6GHz Band Spectrum Measurement System Blocks [17]

The transmission and the receiver can be used alternatively and are shown in figure 4 and 5.

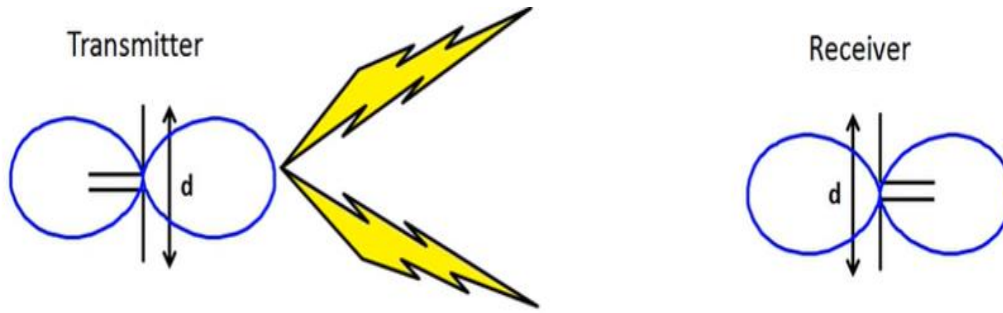


Figure 4: Transmission and receiver of RF setup [17]

A schematic diagram of the antenna is shown in figure 5.

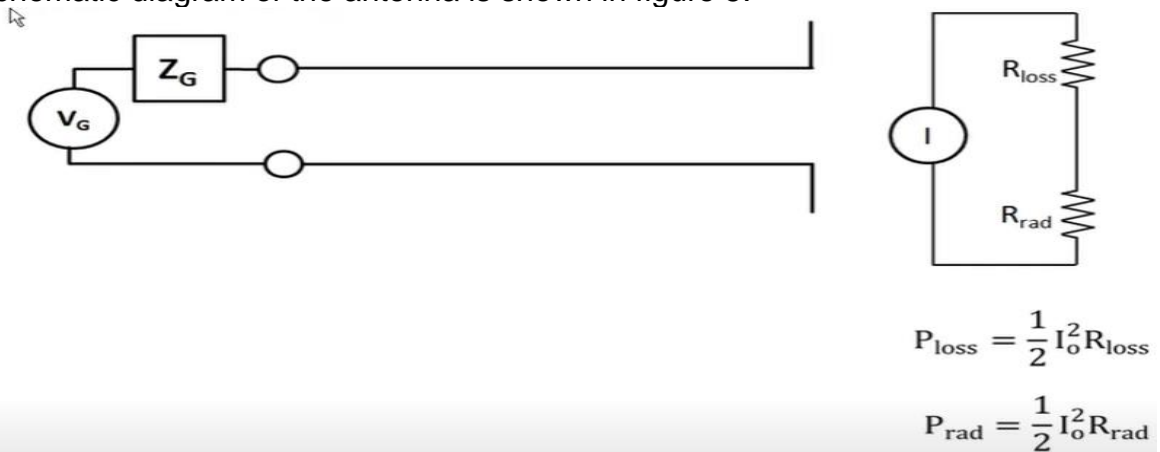


Figure 5: Antenna radiation resistance [17]

Propagation of RF in air is expressed by Frii's transmission equation as

$$\frac{P_{\text{out},r}}{P_{\text{in},t}} = G_t(\theta_t, \phi_t) G_r(\theta_r, \phi_r) \left(\frac{\lambda}{4\pi r}\right)^2 \quad (4)$$

Where $P_{\text{out},r}$ is the power exiting the port of the receive antenna,
 $P_{\text{in},t}$ is the power input at the port of the transmit antenna,
 $G_t(\theta_t, \phi_t)$ is the gain of the transmit antenna, and is a function of the orientation,
 $G_r(\theta_r, \phi_r)$ is the gain of the receive antenna, and is a function of its orientation,
 $\left(\frac{\lambda}{4\pi r}\right)^2$ is the reciprocal of the path loss, calculated from λ , the signal wavelength,
 and the distance between the two antennas.
 coverage respectively.

The radiation intensity from an antenna is given as

$$P_{\text{rad}} = \int_0^{2\pi} \int_0^\pi U_{pk}(\theta, \phi) \sin(\theta) d\theta d\phi = 2\pi A \int_0^\pi \sin^4(\theta) d\theta = A \frac{3\pi^2}{4} \quad (5)$$

Where U_{pk} and A are the areas of receiving or transmission antennas.

The antenna operates as a dipole as shown in figures 6a and 6b

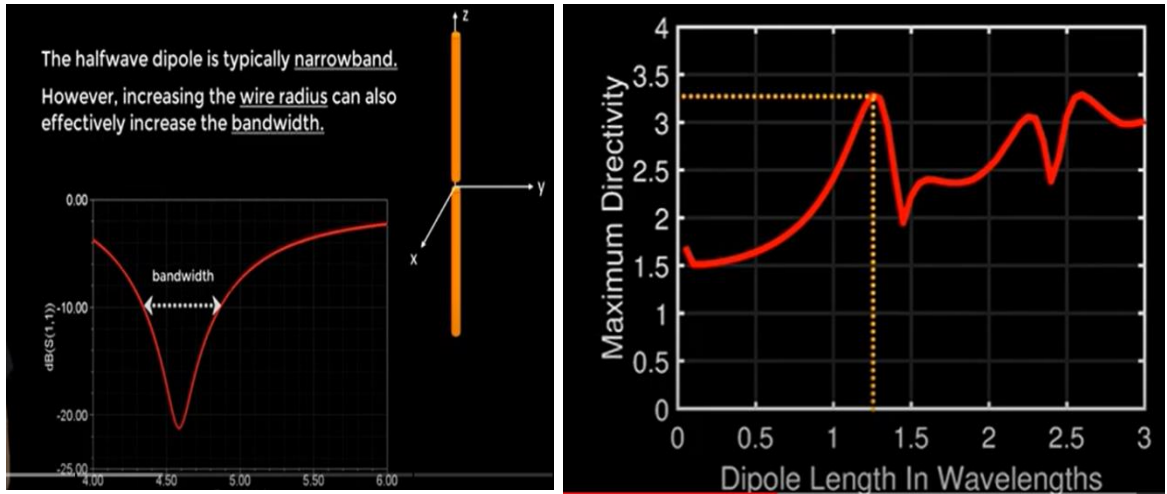


Figure 6a : The half-wave narrow band Figure 6b : Maximum dipole(λ) [17]

The pattern of the RF signal propagates in a spherical form shown in figure 7.

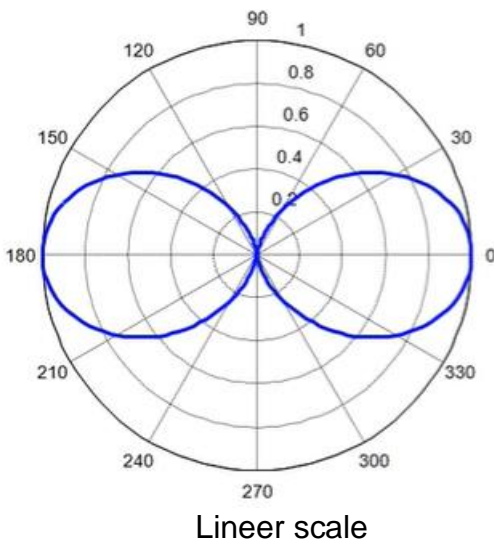


Figure 7 : An antenna pattern of the short dipole [17]

The antenna strength pattern are shown in table 1 and the power density in dB are calculated using equation 6.

Table 1 ; power density at the distance from the centre of the sphere (transmitor) [17]

	P_{end}/P_{start}												
linear	0.001	0.01	0.1	1/5	1/3	1/2	1	2	3	5	10	100	1000

dB	-30	-20	-10	-7	-4.8	-3	0	+3	+4.8	+7	+10	+20	+30
----	-----	-----	-----	----	------	----	---	----	------	----	-----	-----	-----

$$dB \text{ equation: } dB = 10 \log_{10} \left(\frac{P_{end}}{P_{start}} \right) = 20 \log_{10} \left(\frac{E_{end}}{E_{start}} \right) \quad (6)$$

The total RF power radiated per unit area by using Poyting vector was presented in equation 7 below

Unit area ΔA of a sphere in coordinates angles θ, ϕ :

$$\Delta A = r^2 \sin\theta \Delta\theta \Delta\phi \quad (7)$$

Measurement of the power density (dB) were captured by the detector and calculated using equation 8 and 9.

$$P_{rad} = \int_{\theta=0}^{2\pi} \int_{\phi=0}^{\pi} S(r, \theta, \phi) \Delta A \quad (8)$$

$$P_r = r^2 \int_{\theta=0}^{2\pi} \int_{\phi=0}^{\pi} S(r, \theta, \phi) \sin\theta \Delta\theta \Delta\phi \quad (9)$$

Experimental data was collected from Sentec base station at NESREC, Johannesburg in figure 9 and presented in figure 8.

A Fourier transformation was applied to change the RF signal $x(t)$ to a single-tone $(x(f))$, $(-f_1)$ and (f_1) in figure 8.

$X(f)$ can be written as

$$e^{f(\theta)} = \cos(\theta) + j \sin(\theta) \quad (10)$$

$$\cos(\theta) = \frac{e^{j\theta} + e^{-j\theta}}{2} \quad (11)$$

$$\sin(\theta) = \frac{e^{j\theta} - e^{-j\theta}}{2j} \quad (12)$$

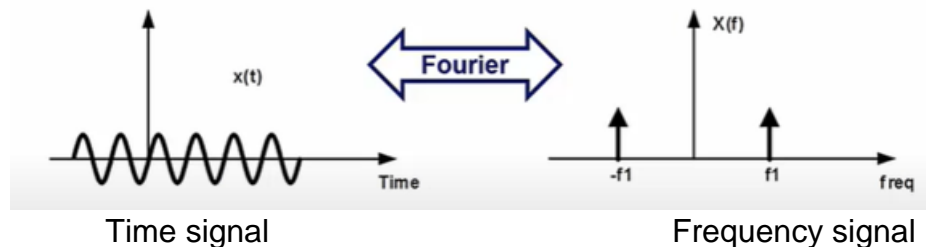


Figure 8 : Time $(x(t))$ and frequency $(x(f))$ RF signal [17]

Table 2: Show the coordinates of the sample collection at NASREC.

Position	Latitude (degree)	Longitude (degree)	Altitude (m)
1	26°24'6.9S	27°98'4.7E	1.738.748
2	26°28'4.3S	27°99'1.2E	1.738.748
3	26°64'3.6S	27°86'7.1E	1.738.748

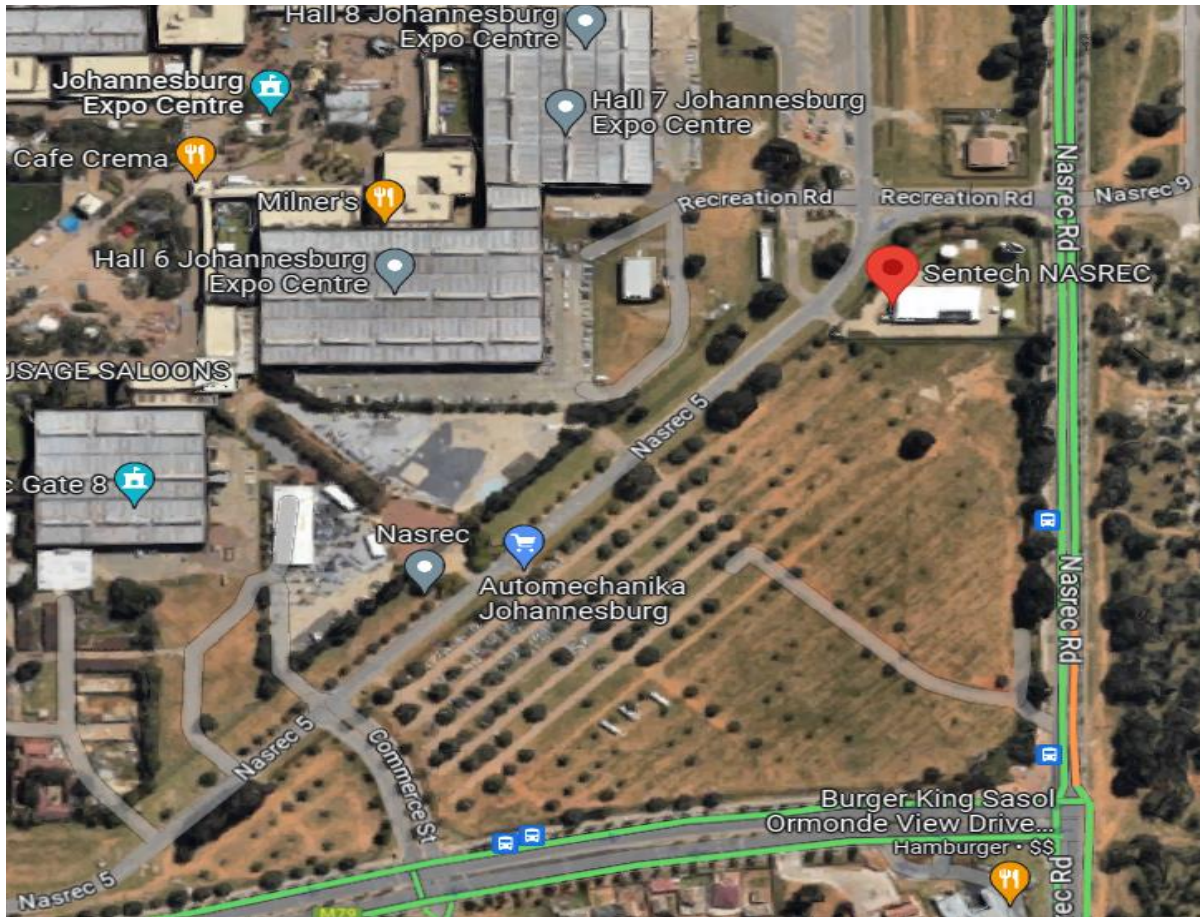


Figure 9 : Sentec 5G radiofrequency station, Johannesburg, South Africa [15]

The detector was equipped with a GPS and was capable of identifying the signals from the satellites. The spectrum analyzer was initialized and allowed sufficient time to reach a stable operational state, The center frequency and span were configured to define the analysis range. To ensure the precision of measurements, the resolution bandwidth (RBW) and video bandwidth (VBW) were appropriately adjusted. Fine-tuning was performed on the amplitude and reference level settings to account for the dynamic range of the signal under examination.

Upon activation of the spectrum analyzer, the frequency spectrum was acquired. Identification and characterization of peaks, signals, noise components, and display features within the spectrum were performed. To quantify critical signal parameters of interest, marker were applied. The acquired spectrum underwent a comprehensive analysis to discern signal attributes, detect anomalies, or identify any interference present in the signal environment.

The 5G Radiofrequency results of SAR $\leq 0.08 \text{ W.kg}^{-1}$ was considered safe.

4 RESULTS AND DISCUSSION

Measurements were conducted at three distinct geographic coordinates. The detector identified the GPS coordinates B02-B37, RF signal in dB from three satellites Galileo, GLONAS and Beidos E02-E25, G03-G32 and the Sentec base station signal R01-R13 Shown as histograms in figures 10,11 and 12 respectively. The *GPS provided the coordinates aligned to the celestial positioning. The signal strength of each satellite and the 5G substation corresponded were detected.*

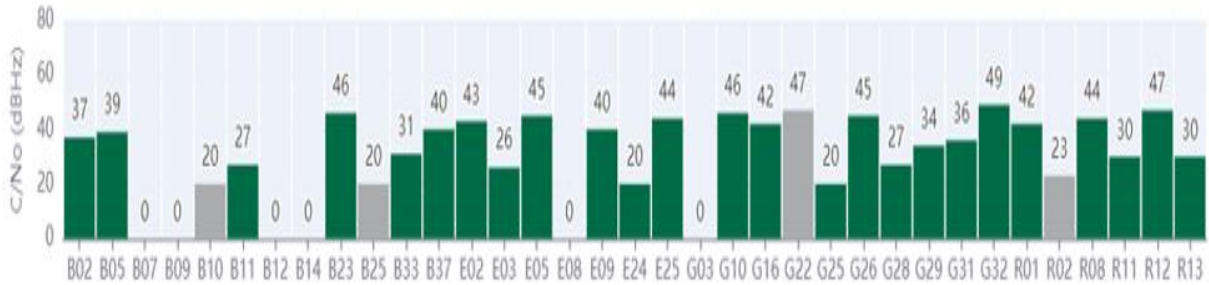


Figure 10: Position 1 pulse obtained inside the generator room

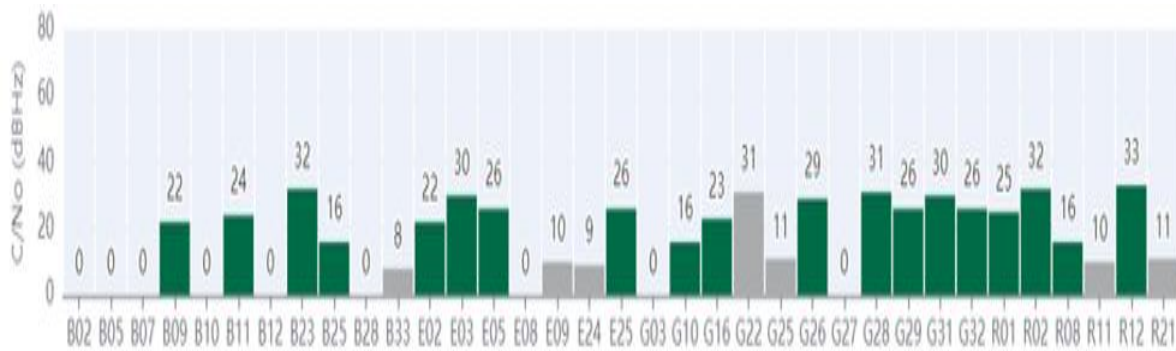


Figure 11: Position 2 pulse obtained 5 meters outside the generation room

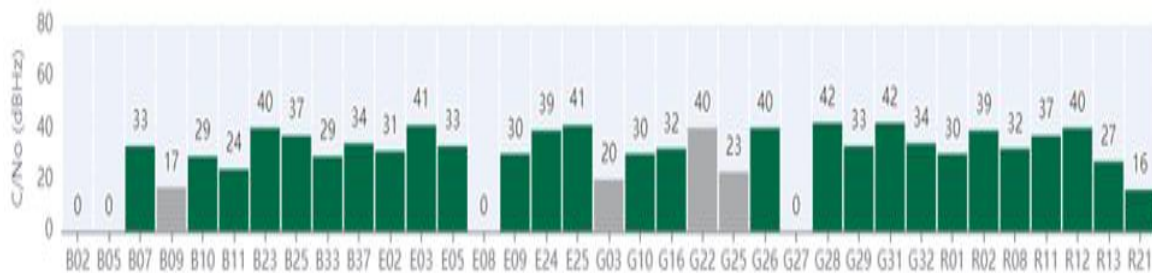


Figure 12: Position 3 pulse obtained 20 meters from the tower

The results demonstrated that RF signal strength was depended on the distance, the angle and the obstacle between the transtitor (base station) and the receiver (detector). The highest signal strength was observed inside the generator room, position 1 table 4. The shorter the distance inside the base station room from the transmitter and the receive, consistant with the inverse square law. Physical barriers and structural elements attenuate RF and played a crucial role in containment of signal propagation to reduce RF eposure below 1.6 W.kg^{-1} [13] limit for non-ionising radiation workers.

The signal strength at 5m distance from the base station outside the room, position 2 table 4. Increasing the distance reduced the distance by the square of the distance

between the transmitter and the receiver. But lower than the RF inside the room. The reduction was due the bigger angle between the transmitter and the receiver next to the base station.

The signal strength at 10m distance from the base station outside the room, position 3 table 4. The RF signal strength was the highest because at that distance the the angle between the transmitter and the receiver was small. The receiver must be place at the maximum RF intensity to ensure uniform and reliable signal coverage throughout research measurement. Additionally, operator/users distance from a tower must comply with the dose limit for the occupational and the member of the public of $1.6W.kg^{-1}$ or $0.08W.kg^{-1}$ respectively.

The frequencies derived from PCI are shown in Tables 2, 3, and 4.

Table 3: Frequency and SSB scan results obtained from position 1

PCI [Beam ID]	SS-RSRP (dBm) ↓	SS-RSRQ (dB)	SS-SINR (dB)	Max TE _{ant} (ns)
1 [6]	-72.01	-10.44	33.39	188
1 [2]	-78.48	-10.92	27.40	188
1 [0]	-79.09	-9.86	26.81	188
1 [5]	-79.57	-13.81	26.63	188
1 [4]	-82.43	-10.73	23.44	188
1 [1]	-84.89	-10.17	21.18	188

Table 4: Frequency and SSB scan results obtained from position 2

PCI [Beam ID]	SS-RSRP (dBm) ↓	SS-RSRQ (dB)	SS-SINR (dB)	Max TE _{ant} (ns)
1 [2]	-58.23	-10.39	39.35	324
1 [3]	-59.11	-10.22	37.94	324
1 [5]	-60.43	-10.28	39.74	324
1 [6]	-60.67	-9.38	38.77	324
1 [1]	-64.12	-10.39	36.17	324
1 [0]	-73.41	-10.00	28.85	324

Table 5: Frequency and SSB scan results obtained from position 3

PCI [Beam ID]	SS-RSRP (dBm) ↓	SS-RSRQ (dB)	SS-SINR (dB)	Max TE _{ant} (ns)
2 [5]	-59.93	-9.37	35.12	228
2 [6]	-61.08	-9.78	33.99	228
2 [4]	-63.00	-9.71	34.51	228
2 [0]	-68.60	-9.24	32.47	228
2 [1]	-70.44	-9.78	29.96	228
2 [3]	-70.46	-9.74	31.67	228
2 [2]	-73.23	-9.40	29.20	228

The signal frequency results of 3488.74 ± 20.60 MHz i.e., 3.5GHz from a direct digital modulation of an RF receiver for positions 1, 2, and 3, and the delta frequency of 1159.00 ± 21 b/s i.e., $1.2\text{Gb/s} \pm 21$ b/s were obtained. The average pulse time of 247 ± 57.07 ns. These results were within a low-power, wideband wireless of 1.2Gb/s as prescribed for the 5G range. The delta amplitude for the setup was -1.53 ± 2.81 db demonstrating a gain of RF reaching the receiver.

Figures 13, 14, and 15 showed the RF spectra obtained from positions 1, 2, and 3, respectively. The real peak was identified by marker 1 at the centre of the the main graph which represent the centre of the dipole antenna. The other two small peaks on either side of the real peak represent the negative frequencies.

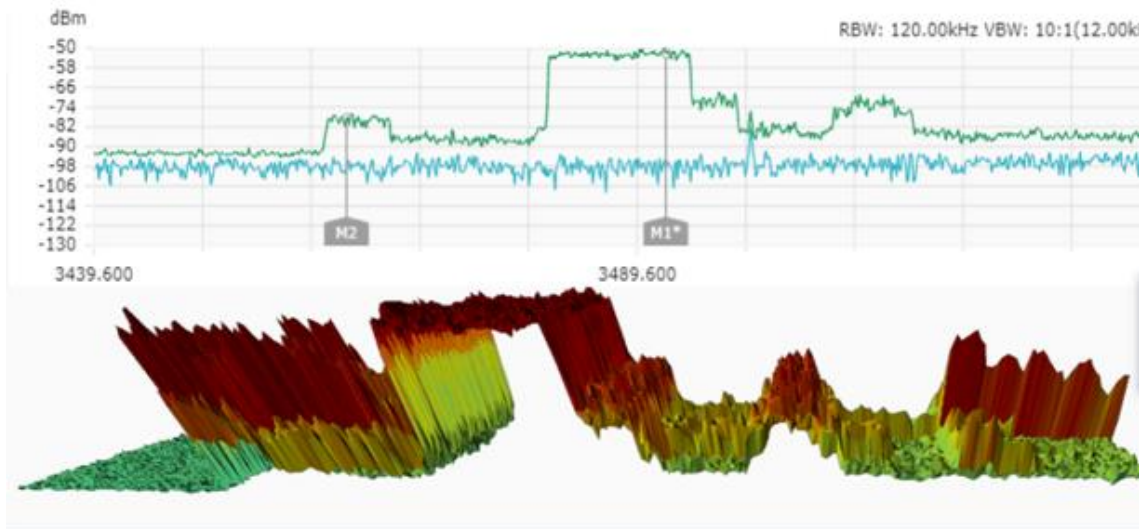


Figure 13: Spectrum analysis obtained from position 1

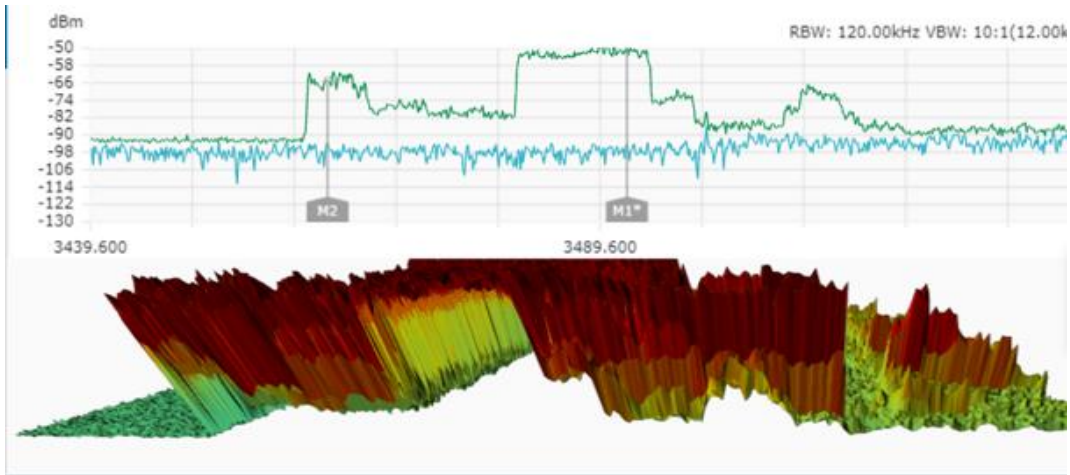


Figure 14: Spectral analysis obtained from position 2

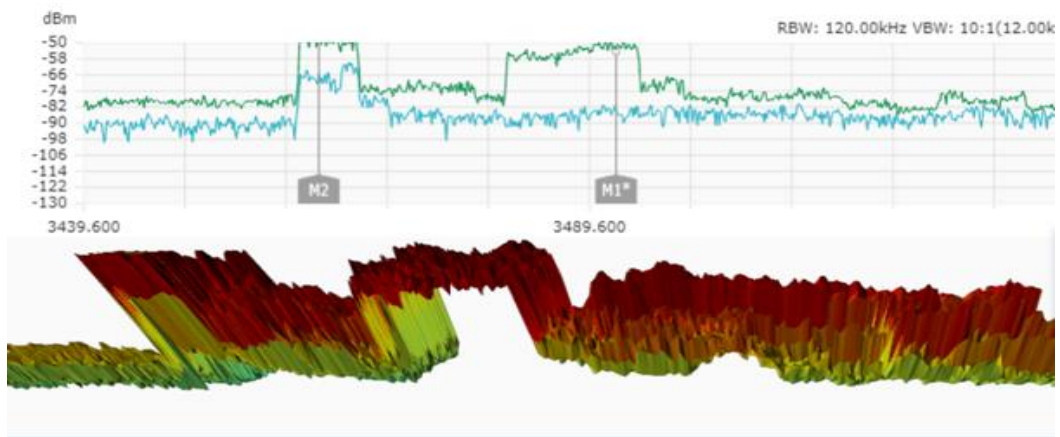


Figure:15 Spectral analysis obtained from position 3

The real-time RF signals are shown in Figures 16, 17, and 18.

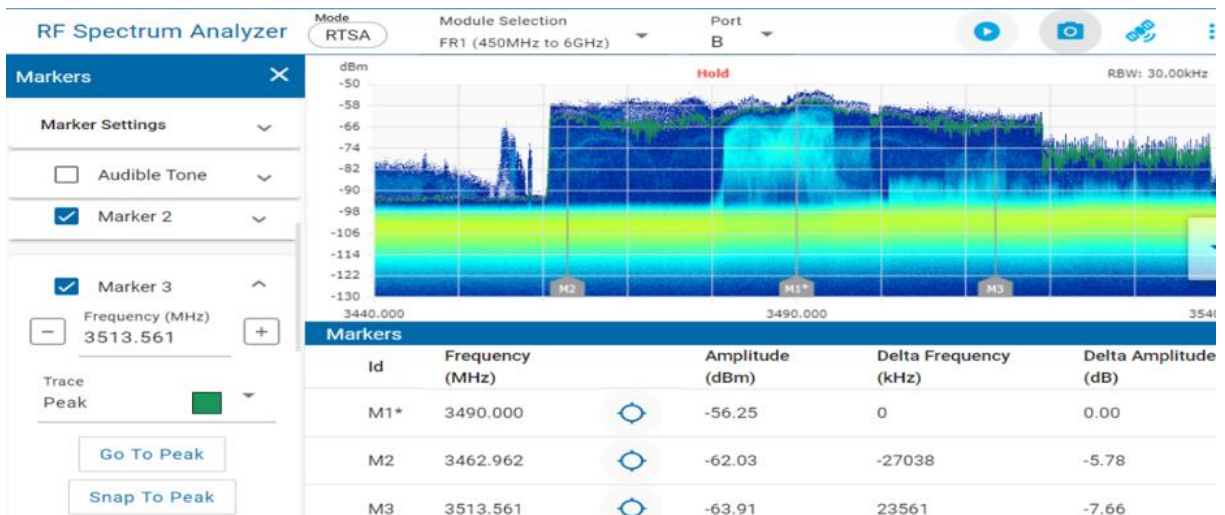


Figure 16: Real-time RF spectrum obtained from position 1

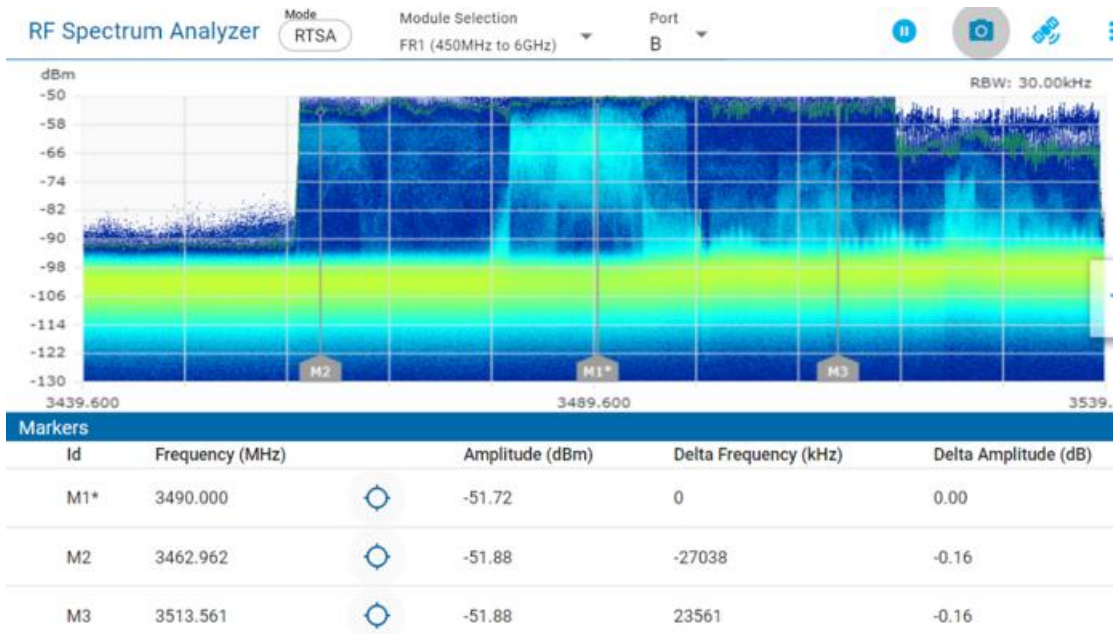


Figure 17: Real-time RF spectrum obtained from position 2



Figure 18: Real-time RF spectrum obtained from position 3

The 5G Analyzer a scientific approach to analyze and characterize the 5G signals, as illustrated in Figures 16, 17, and 18. This advanced analytical tool offered an array of functionalities, including beamforming metrics, enabling the assessments of up to 64 beams. Furthermore, it exhibited the ability to delineate the 12 most robust beams, accompanied by precise power measurements for each.

The strength of 5G RF signals (dB) and the power density (Watts) are presented in Table 4.

Table 4: RF (dB) and Energy (Watts) per position

Position 1		Position 2		Position 3	
dB	W	dB	W	dB	W
33,39	2,18	39,35	8,60	35,12	3,25
27,40	5,50	27,95	6,24	33,99	2,51
26,81	4,80	39,74	9,42	34,51	2,81
26,63	4,60	38,77	7,53	32,47	1,77
23,44	2,21	36,17	4,14	29,96	9,91
21,18	1,31	28,85	7,67	31,67	1,47
26,29±4.12	3,43±1.59	35,14±4.91	7,27±1.71	32,95±1.78	3,62±2.88

The average magnitude of the electromagnetic energy of 4.77 ± 2.77 Watts was calculated from columns 2, 4, and 6 in Table 4 which was measured from three sample positions 1, 2, and 3 respectively. These findings provided valuable insight into the safety of human beings who are subjected to various electronic devices and infrastructures that utilize radiofrequency radiation at those positions indicated above. The average specific absorption rate (SAR) in watts in this study for an average 60kg man was 0.08 W.kg^{-1} which is equal to SAR limits for general population/uncontrolled exposure of 0.08 W.kg^{-1} [13] averaged over the whole body, and a peak spatial-average SAR of 1.6 W.kg^{-1} averaged over any 1 gram of tissue (defined as a tissue volume in the shape of a cube) [13]. This information is essential for understanding the potential thermal effects on the human body, as power levels can influence the rate at which tissue absorbs energy. On average, individuals with a weight of 60 kilograms should not exceed the recommended safety threshold energy of 0.08 W.kg^{-1} for whole-body exposure [13] [15]. This study has shown that the measured SAR is consistent with established safety limits and reassuring safety for the general population's exposure to radiofrequency radiation.

5 CONCLUSION

In conclusion, this study provided valuable insights into the assessment of average power and specific absorption rate (SAR) and is consistent with SAR limits recommended for the general population/uncontrolled exposure, as specified by regulatory bodies such as the International Commission on Non-Ionizing Radiation Protection (ICNIRP) [13] and the Institute of Electrical and Electronics Engineers (IEEE) [14] which affirm the safety of the tested conditions.

The research findings complied with the established safety standards and the importance of adhering to international guidelines in mitigating potential health risks associated with electromagnetic exposure. These findings provided reassurance of the examined sample positions and power levels which fell well within the safety SAR parameters of $\leq 0.08 \text{ W.kg}^{-1}$ established by the ICNIRP and IEEE, ensuring that the individuals who are exposed to similar conditions are not at risk of adverse effects. This current study results contributed to the growing evidence supporting the safe practices and guidelines in the field of non-ionizing radiation and ultimately the safety of the members of the public.

Ongoing research is underway on volunteers to determine the cell membrane permeability, chromosomal aberration (DNA), and nucleon changes due to 5G radiofrequency. The results will be compared with the SAR results.

6 BIBLIOGRAPHY

- [1] Rappaport, T. S., Sun, S., Mayzus, R., Zhao, H., Azar, Y., Wang, K., & Shafi, M. (2013). Millimeter wave mobile communications for 5G cellular: It will work! *IEEE Access*, 1, 335-349. DOI: [10.1109/ACCESS.2013.2260813](https://doi.org/10.1109/ACCESS.2013.2260813)
- [2] Pi, Z., Khan, F. U., & Kousaridas, A. (2015). Beamforming for millimeter-wave communications: An inclusive survey. *IEEE Communications Surveys & Tutorials*, 18(2), 949-973.
- [3] Agilent Technologies. (2017). Fundamentals of Real-Time Spectrum Analysis. Retrieved from <https://www.keysight.com/us/en/assets/7018-04190/application-notes/5992-1774.pdf>
- [4] Rohde & Schwarz. (2020). Fundamentals of Spectrum Analysis. Retrieved from https://www.rohde-schwarz.com/us/applications/fundamentals-of-spectrum-analysis-application-card_56280-940496.html
- [5] Federal Communications Commission (FCC). (2021). Spectrum Dashboard. Retrieved from <https://www.fcc.gov/spectrum-dashboard>
- [6] Asadi, A., Wang, Q., Mancuso, V., & Gupta, R. (2014). A survey on device-to-device communication in cellular networks. *IEEE Communications Surveys & Tutorials*, 16(4), 1801-1819.
- [7] Godpower I. Akawuku, Obioma Peace, Samuel I. Udobi, "5G Technology and its Health Impact in Africa", *Idosr Journal of Computer and Applied Science* 5(1):43-51, 2020, I SN: 2579-0803.
- [8] Fiorella Belpoggi, "Health Impact of 5G", ISBN: 978-92-846-8030-6, doi: [10.2861/657478](https://doi.org/10.2861/657478), 2021.
- [9] Mark Holker CEng FIEE MBIM, In *Telecommunications Engineer's Reference Book*, 1993.
- [10] Ken Karipidis, Rohan Mate, David Urban, Rick Tinker, and Andrew Wood, "5G Mobile networks and health – a state of the science review of the research into low-level RF fields above 6 GHz", *Journal of Exposure Science & Environmental Epidemiology* (2021) 31:586-605, <https://doi.org/10.1038/s41370-021-00297-6>.
- [11] Luca Chiaraviglio, Senior Member, IEEE, Ahmed Elzanaty, Member, IEEE, and Mohamed-Slim Alouini, Fellow, IEEE, "Health Risks Associated with 5G Exposure: A View from the Communications Engineering Perspective", June 2020.
- [12] Valberg PA, Emilie van Deventer T, Repacholi MH. Workgroup Report: Base Stations and Wireless Network – Radiofrequency (RF) Exposures and Health Consequences. *Environ Health Perspect* 115:416-424 (2007). doi:10.1289/ehp.9633 available via <http://dx.doi.org/>
- [13] International Commission on Non-Ionizing Radiation Protection (ICNIRP), "ICNIRP guidelines on limiting exposure to time-varying electric, magnetic and electromagnetic fields (100 kHz to 300 GHz)", Jul.2020 Available at: <https://www.icnirp.org/cms/upload/publications/ICNIRPPrfgdl2020.pdf>,
- [14] "C95.1-2019 IEEE standard for safety levels concerning human exposure to radiofrequency electromagnetic fields, 3 kHz to 300 GHz, "Institute of Electrical, Electronics and Engineers (IEEE), New York, NY, US, Tech. Rep., 2019.

- [15] <https://www.google.com/maps/@-26.2440283,27.9861993,757m/data=!3m1!1e3!5m1!1e1?entry=ttu;>
- [16] <http://dspace.mit.edu/handle/1721.1/7582>
- [17] [http://www.amanogawa.com/archive/DipoleAnt-2.html;](http://www.amanogawa.com/archive/DipoleAnt-2.html)
- [18] [https://www.scribd.com>3-5GHz.Attena;](https://www.scribd.com>3-5GHz.Attena)